Ingeniería
Investigación y
Tecnología

Analysis of nonlinear gas turbine models using influence coefficients

Análisis de los modelos no lineales de turbinas de gas a través de los coeficientes de influencia

González-Castillo Iván

Instituto Politécnico Nacional

Escuela Superior de Ingeniería Mecánica y Eléctrica Culhuacán

E-mail: chrivangc@gmail.com

https://orcid.org/0000-0002-0730-546X

Loboda Igor

Instituto Politécnico Nacional

Escuela Superior de Ingeniería Mecánica y Eléctrica

E-mail: iloboda@gmail.com

https://orcid.org/0000-0002-4442-5540

Abstract

The limited availability of gas turbine data, especially fault data, and the high costs and risks of experimenting with faults in test benches cause the lack of data to form a representative fault classification for gas turbine diagnostics. These circumstances explain the need of models that can simulate the faults. The utility of the simulated data for the diagnostics depends on the accuracy of fault simulation at different operating modes. The present paper analyses random errors of and an operating conditions influence on a gas turbine fault description. The analysis is applied to the thermodynamic models of a turboshaft and a turbofan of the well-known commercial software GasTurb 12. Big data containing measured quantities with the influence of fault parameters and operation conditions were generated with this software. Then the matrixes that determine the influence of faults and operating conditions were calculated to analyze the accuracy and behavior of the models. The results show that the engine models are accurate enough and the influence of operation conditions on the fault action is significant in contrast to some other engine models.

Keywords: Turbofan, turboshaft, nolinear models, influence coefficients.

Resumen

La poca disponibilidad de datos reales de turbinas de gas, sobre todo de fallas, y los altos costos y riesgos de utilizar bancos de pruebas para obtenerlos ocasionan que rara vez se tengan datos estadísticamente representativos para formar una clasificación de fallas para el diagnóstico de turbinas. Estas circunstancias explican la necesidad de desarrollar modelos que puedan simular las fallas de las turbinas de gas. La utilidad para el diagnóstico de los datos simulados dependerá de la precisión de la simulación de fallas en diferentes regímenes. El artículo presentado analiza los errores aleatorios de la descripción de las fallas y la influencia de condiciones de operación a esta descripción. El análisis se aplica a los modelos termodinámicos de un turbo eje y un turbo ventilador del conocido software GasTurb 12. Datos extensos con la influencia de los parámetros de falla y condiciones de operación fueron generados por GasTurb 12. Entonces las matrices con la influencia de las fallas y las condiciones de operación se calcularon para analizar la precisión y comportamiento de los modelos. Los resultados muestran que los modelos de los motores son suficientemente precisos y la acción de fallas depende significativamente de las condiciones de operación.

Descriptores: Turbo ventilador, turbo eje, modelos no lineales, coeficientes de influencia.

Introduction

During maintenance, gas turbine performances are affected by different abrupt and gradual faults. Their main sources are: Fouling, corrosion, erosion, worn seals, object damage and increased blade tip clearance. The information on these faults and their consequences can be found in (Fentaye *et al.*, 2019 and Tahan *et al.*, 2017). Fault manifestations are rare in real engines and therefore their mathematical models are involved in fault description. These models present the relationship between gas path variables (pressures, temperatures, fuel flow rate, power, etc.), component performances, and operating conditions (ambient and power set variables) that are formed through thermodynamic equations and conservation laws (Vanini *et al.*, 2014) or by using empiric information. The models offer an effective way of better understanding engine behavior and identifying the sources of engine performance degradation. The models can be used to calculate nominal values of measured variables corresponding to a healthy engine. Knowledge of these values allows determining the measurement deviations of an actual engine. Moreover, the models help with describing the influence of each fault on the measurements and, in this way, help to form a fault classification. Thus, the gas turbine models constitute the basis for the diagnostic algorithms (Jardine *et al.*, 2006).

There are two general types of gas turbine models. The first type includes physics-based models that are developed by using the laws of conservation of matter, momentum and energy through the gas path. Some of the most well-known software such as GasTurb, GSP and NASA's C-MAPSS were developed with these principles. The second type models are known as "black boxes" or data-driven model. These models consist exclusively of the mathematical relationships between the input parameters and the output variables, regardless of the physical process and the laws that govern it. Various techniques of artificial intelligence, such as neural networks, and approximation functions, for example, polynomial regression, have been used to create data-driven models of gas turbines. The precision of the models depends on many factors, among them, the accuracy of engine components performance description.

According to operating and health conditions, the simulation includes two options: design-point simulation and off-design analysis. The design-point simulation is performed at the single operating point that will be mostly used in real engine operation and at which the engine has the best performances. This simulation allows the designer to choose the best configuration of a new engine. The off-design analysis helps an engine operator to know engine performances at different operating points and under different health conditions. For the purpose of diagnostics, the latter is usually applied.

Gas turbines and their components can also have different levels of description in space resulting in 0-D, 1-D, 2-D, and 3-D model types (North Atlantic Treaty Organisation, 2002). The most profound description is typical for design-point simulation during engine design. The 0-D models compute averaged gas flow variables at discrete stations, mainly at inputs and outputs of engine components (compressors, turbines, burners, nozzles, inlet and outlet devices, etc.). The gas turbine diagnostics usually employs the 0-D models because they are relatively simple and allow describing the behavior of a whole engine (Kamboukos & Mathioudakis, 2005).

The software packages for gas turbine simulation usually do not have a friendly interface and require qualified personnel. To avoid this difficulty, Dr. Joachim Kurzke has developed since the early 90's the software GasTurb (GasTurb GmbH, 2015). This software hides the mathematics from the user and has an intuitive interface. The GasTurb 12 simulation has the on-design or off design options and can be characterized as physics-based and 0-D. It has the capability of many different calculations for all main gas turbine schemes and applications.

The errors of physics-based models, like the models of GasTurb 12, depend on the uncertainties in the description of two dependences: dependency of gas path variables from operating conditions and dependency of these variables from special fault parameters that are introduced into the model to take into consideration an engine health condition. These parameters slightly shift the performances of engine components (compressor, burner, turbine, etc.) thus reflecting the influence of different component faults. All of the error sources must be known to determine a total model uncertainty (Holst, 2012). One of the ways to estimate the model errors is the analysis of the coefficients of the influence of engine faults and operating conditions on gas path variables.

Loboda *et al.* (2007) have analyzed the behavior of the fault influence coefficients of an industrial power plant and an aircraft engine. They conclude that, when these coefficients do not significantly change from one operating point to another, an universal fault classification can be used that makes gas turbine diagnosis much more feasible; otherwise, if the change is considerable, a multipoint diagnostic option has additional advanta-

ge. Additionally, the authors noted elevated random errors in the computed coefficients. Such errors cause misdiagnosis and should be maximally reduced. This reasoning shows why it is important to know the behavior of influence coefficients before the development of engine diagnostic algorithms.

This paper deals with the influence coefficient analysis of a popular gas turbine simulation software GasTurb 12. Because of its popularity and a long history of development, this software may have a high computational accuracy and may be used as an accuracy pattern for another gas turbine simulation programs. On the other hand, since GasTurb 12 allows simulating different engine schemes, the influence coefficient analysis is repeated in the paper for two different engines, turboshaft and turbofan. This will help with drawing more general and grounded conclusions. Gas path variables depend on both faults and operating conditions, therefore a linear engine model includes two corresponding matrixes named a fault influence matrix H and an operating condition influence matrix G. Section 2 presents the methodology of computing both matrixes. In section 3, we firstly determine the optimal value of fault parameters variation to compute the matrix H. Once the optimal variation was selected, the influence of the operating conditions on the matrix H is evaluated. In the same way, section 4 performs the analysis of the matrix G.

Methodology of the analysis of influence coefficients

Gas path analysis

A physics-based model (thermodynamic model) constitutes the bases of one of the principal gas turbine diagnostic approaches called Gas Path Analysis (GPA). Using the model, the approach aims to estimate a health condition of each engine component.

At gas turbine steady states, engine gas path variables (fuel mass flow rate, thrust or power, gas path pressures and temperatures, etc.) depend on operating conditions (power set parameters and ambient conditions) and engine health parameters that determine actual component performance maps. Generally presented by a nonlinear physics-based static model, the relationship between the dependent variables (monitored variables) and the independent parameters is highly non-linear (Li, 2002). The model is formed using gas path thermodynamic equations and conservation laws and is also called a thermodynamic model. Within the model, an (m×1)-vector $\vec{Y}$ of monitored variables is computed employing as arguments engine operational

conditions joint in an (s×1)-vector $\vec{U}$ and engine health parameters united in an (r×1)-vector $\vec{\theta}$. Given the above explanation, the thermodynamic model can be expressed by the following nonlinear dependency between the mentioned vectors (Urban, 1973):

$$\vec{Y} = F(\vec{U}, \vec{\theta}) \qquad (1)$$

This physics-based model has many uses. First, it allows simulating many fault scenarios and creating a fault classification (Loboda *et al.,* 2007). Second, the model is the basis of GPA that involves nonlinear system identification techniques for the estimation of the parameters $\vec{\theta}$ (Pinelli & Spina, 2002). These techniques look for those parameters that provide the best tuning of the model to the measurements of a particular engine. Third, the thermodynamic model helps with forming many simplified models (Sampath & Singh, 2005), like a linear model given by:

$$\delta\vec{Y} = H\delta\vec{\theta} + G\delta\vec{U} \qquad (2)$$

This static model is linearization of eq. (1). A vector of fault parameters $\delta\vec{\theta}$ presents relative changes of the health parameters induced by engine degradation, and a vector $\delta\vec{U}$ denotes relative changes of operating conditions. Matrixes H and G are constituted from influence coefficients for the corresponding fault parameters and operating conditions. Within a linear GPA, the use of the linear model makes it possible to estimate parameters $\delta\vec{\theta}$ by simple analytical expressions, as proposed in (Urban, 1973) upon the assumption of no variations in the operating conditions.

One can see in eq. (2) that the mode of the influence on the monitored variables is the same for the fault parameters and the operating conditions i.e. through constant influence coefficients of the corresponding matrixes. Therefore, in addition to the matrix H, the matrix G may be a good indicator of the errors of the thermodynamic model, and we include the matrix G into our analysis as well.

Computation of influence coefficients

The fault influence matrix H is composed from the coefficients of the influence of small relative changes $\delta\vec{\theta}$ on the respective changes of the monitored variables when operating conditions do not change. The matrix is usually calculated using the thermodynamic model given by eq. (1). First, the monitored quantities $\vec{Y}$ are computed with nominal health parameters $\vec{\theta}_0$ corresponding to a healthy engine at a given operating

point determined by a constant value of a power set variable. Small increase $\Delta\theta_j$ is then added independently to each health parameter and the computation of $\bar{Y}(\theta_{j0} + \Delta\theta_j)$ is made once more with the same power set variable value. Given the known values of a monitored variable Y_i and a health parameter θ_j, the respective influence coefficient is finally calculated by:

$$H_{ij} = \frac{\delta y_i}{\delta\theta_j} = \frac{Y_i(\theta_{jo} + \Delta\theta_j) - Y_i(\theta_{jo})}{Y_i(\theta_{jo})} \Big/ \frac{\Delta\theta_j}{\theta_{jo}} \qquad (3)$$

This calculation is illustrated by Figure 1. As the variation $\Delta\theta j$ decreases, the coefficient H_{ij} approaches the corresponding partial derivative.

Having been computed, the influence coefficients constitute the [m×r]-matrix of fault influence as is shown below.

$$H = \begin{bmatrix} \dfrac{\delta Y_1}{\delta\theta_1} & \dfrac{\delta Y_1}{\delta\theta_2} & \cdots & \dfrac{\delta Y_1}{\delta\theta_r} \\ \dfrac{\delta Y_2}{\delta\theta_1} & \dfrac{\delta Y_2}{\delta\theta_2} & \cdots & \dfrac{\delta Y_2}{\delta\theta_r} \\ \vdots & \vdots & \ddots & \vdots \\ \dfrac{\delta Y_m}{\delta\theta_1} & \dfrac{\delta Y_m}{\delta\theta_2} & \cdots & \dfrac{\delta Y_m}{\delta\theta_r} \end{bmatrix} \qquad (4)$$

The accuracy of the matrix elements H_{ij} computed according to eq. (3) depends on variation value $\delta\theta_j$. On the one hand, to reduce linearization errors, the variation value should be small. On the other hand, it should not be too small to avoid significant influence of the errors of numerical calculation of variables Y. For example, if $\delta\theta_j$ results in $Y_i(\theta_j) - Y_i(\theta_{jo}) / Y_i(\theta_{jo}) = 0.01$ and numerical errors of $Y_i(\theta_j)$ and $Y_i(\theta_{jo})$ are equal to 10^{-5}, then an error of H_{ij} will be $\sqrt{2} \cdot 10^{-5}/0.01 = 1.41 \cdot 10^{-3}$ i.e. 141 times greater than the error of Y. The above reasoning explains the need to look for the optimal variation value.

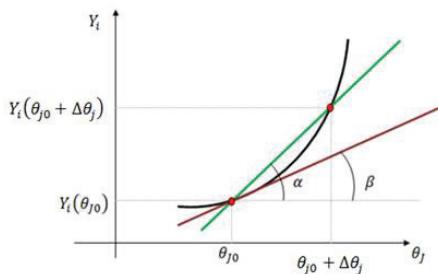The matrix G in eq. (2) presents the influence of operating conditions. This matrix is determined in the simi-

lar way as the matrix H. Its elements are calculated according to the following expression:

$$G_{ij} = \frac{\delta Y_i}{\delta U_j} = \frac{Y_i(U_j) - Y_i(U_0)}{Y_i(U_0)} \Big/ \frac{U_j - U_{0j}}{U_{0j}} \qquad (5)$$

Once all the elements are computed, the [m×r]-matrix of operating condition influence takes the form:

$$G = \begin{bmatrix} \dfrac{\delta Y_1}{\delta U_1} & \dfrac{\delta Y_1}{\delta U_2} & \cdots & \dfrac{\delta Y_1}{\delta U_s} \\ \dfrac{\delta Y_2}{\delta U_1} & \dfrac{\delta Y_2}{\delta U_2} & \cdots & \dfrac{\delta Y_2}{\delta U_s} \\ \vdots & \vdots & \ddots & \vdots \\ \dfrac{\delta Y_m}{\delta U_1} & \dfrac{\delta Y_m}{\delta U_2} & \cdots & \dfrac{\delta Y_m}{\delta U_s} \end{bmatrix} \qquad (6)$$

INFLUENCE COEFFICIENT BEHAVIOR AND ERRORS

Loboda *et al.* (2007) have analyzed the behavior of the fault influence coefficients of an industrial power plant and an aircraft engine. Figure 2 illustrates this analysis by presenting the plots of different influence coefficients vs. operating points (steady states). As follows from Figure 2a, the level of the coefficients of the industrial power plant does not significantly change for different operating points, but there are some random perturbations in the coefficient behavior. For the aircraft engine presented in Figure 2b, it can be stated that some coefficients have a more significant general trend in the comparison with the power plant case, while the level of random perturbations is approximately the same, excepting the spike in point 26. However, this spike is caused by a normal opening of a compressor bypass valve and cannot be considered as a simulation error. The analysis of the thermodynamic models employed to compute the influence coefficients reveals that the random errors they mainly appear from not accurate enough approximation of engine component performances.

The analysis given in the rest of the present paper has the following purposes. First, it is necessary to ascertain whether the random fluctuations observed in Figure 1 are an intrinsic property of any thermodynamic model or they can be eliminated. Second, the matrix G is also a derivative matrix, and it is of practical interest to verify whether its coefficients have random errors. Third, some diagnostic methods are based on the assumption that changing operating condition do not significantly influence on influence coefficient values i.e. the impact of faults is not considerably affected

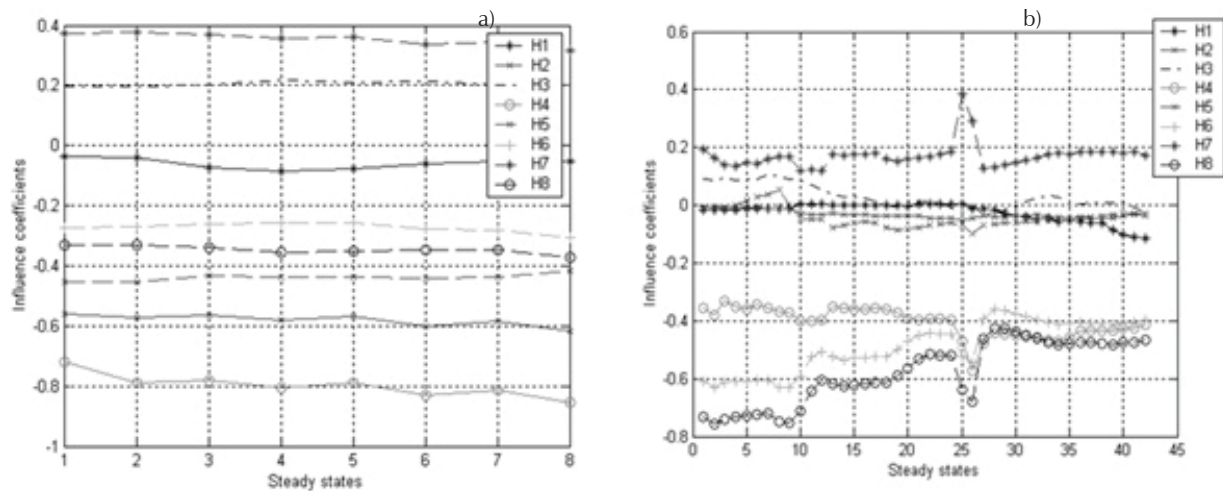Figure 1. Numerical calculation of the matrix H coefficients

Figure 2. Fault influence coefficients versus steady states given by fuel consumption as a power set variable: a) coefficients of the influence of 8 fault parameters on the power turbine temperature of the industrial power plant; b) coefficients of the influence of 8 faults on the intermediate pressure turbine temperature of the aircraft engine (Loboda *et al.*, 2007)

by an engine regime. To the contrary, in multipoint algorithms a diagnostic accuracy is improved if the operating condition influence is significant. Therefore, in this paper a general dependence of influence coefficients from operating conditions will also be evaluated. To see all the details of the influence coefficient behavior, a graphical mode is very useful. To draw well-grounded and general conclusions, we will analyze plots of different elements of both influence matrices of two engines.

Analyzed quantities of test case engines

The models of a turboshaft and a turbofan of the Gas-Turb 12 software were selected to conduct the analysis of the matrices H and G. Table 1 specifies the quantities considered in both engines. These quantities determine the structure of the matrixes: turboshaft [8×6]-matrix H, turbofan [8×5]-matrix H, and [8×2]-matrixes G of both engines. During the matrixes computation, a spool speed (ZXN or ZXNH) is employed as a power set variable. In the section below, we will analyze the fault influence matrixes H of both engines. We firstly will find the optimal variation value for the fault parameters $\delta\theta$, as well as the operating conditions U. The optimal value provides the highest accuracy of the corresponding matrix and linear model. Once the mentioned value is found, each influence matrix will be computed under different operating conditions, and the impact of the operating conditions on the behavior of the matrix elements will be estimated.

Analysis of the fault influence matrix

Firstly, in the next subsection we will find the optimal variation values for the fault parameters $\delta\theta$ for the turboshaft and turboprop. These values mean the highest accuracy of the matrix H computation. Once the mentioned values are found, the matrixes H necessary for our analysis will be calculated and the influence of the operating conditions on the matrix elements will be estimated.

Optimal variation value of fault parameters

In order to find the optimal variation value of fault parameters, we computed matrixes H with different levels of the variation. The simulation was performed in GasTurb 12 with six fault parameters for the turboshaft and seven for the turbofan. First, a healthy engine (when $\overline{\delta\theta} = 0$) was simulated. Its performance is labeled as "design point". Then, many off design points were simulated when the engine model had different values of each fault parameter varying independently. In Figure 3 the mentioned points are shown in the compressor map of the turbo shaft.

Conventionally, maximum value of 0.05 to 0.07 (5 to 7 %) is considered for the fault parameters (Fentaye *et al.*, 2019). For this reason, a total range of the variation was approximately limited by 0.1 for both engines. To better present the behavior of the influence coefficients, the range was divided into three intervals with individual variation increment in each one. In total, 285 variation values of each fault parameter were introduce one

Table 1. Fault parameters, monitored variables and operating conditions

No.	Turboshaft		Turbofan	
	Fault parameters (θ)			
1	Compressor capacity [%]	CC	Low pressure compressor (LPC) capacity [%]	LPCC
2	Compressor efficiency [%]	CE	High pressure compressor (HPC) capacity [%]	HPCC
3	High pressure turbine (HPT) capacity [%]	HPTC	HPC efficiency [%]	HPCE
4	HPT efficiency [%]	HPTE	HPT capacity [%]	HPTC
5	Power turbine (PT) capacity [%]	PTC	HPT efficiency [%]	HPTE
6	PT efficiency [%]	PTE	-	-
	Monitoried Variables (Y)			
1	Shaft power delivered [kW]	SPD	Net thrust [kN]	NT
2	Fuel flow [kg/s]	FF	Specific fuel consumption [g/(kN*s)]	SFC
3	Compressor exit pressure [kPa]	P3	HPC exit pressure [kPa]	P3
4	HPT exit pressure [kPa]	P44	HPT exit pressure [kPa]	P44
5	PT exit pressure [kPa]	P5	LPT exit pressure [kPa]	P5
6	Compressor exit temperature [K]	T3	HPC exit temperature [K]	T3
7	HPT exit temperature [K]	T44	HPT stator outlet temperature [K]	T41
8	PT exit temperature [K]	T5	LPT exit temperature [K]	T5
	Operating conditions (U)			
1	Input temperature	T1	Inlet temperature	T2
2	HPC spool speed	ZXN	HPC spool speed	ZXNH

by one in the turboshaft model. The monitored variables and matrices H were computed for each value. For the turbofan, the number of considered variation values and the resulting matrices was 294.

Table A1 of the Appendix section illustrates the set of variation values for the turboshaft and presents the corresponding influence coefficients of a compressor efficiency fault parameter. For this engine, Figure 4 shows the semi logarithmic graphs of the coefficients of influence of the same fault parameter on all the monitored variables (these coefficients constitute a column in the matrix H). According to the behavior of the coefficients, a total span of the fault parameter variation can be divided into four intervals. In the first interval, the fault parameter variations are too small, and the engine model of GasTurb 12 does not react to these variations. The second interval is characterized by significant random perturbations in the influence coefficients because of numerical errors of the simulation in GasTurb. In the third interval, the coefficients are practically constant. In the fourth interval, the coefficients begin to change significantly because of linearization errors. Given such a behavior of the coefficient, the third interval presents proper fault parameter variations. The other influence coefficients of the matrix H show similar behavior, and a common variation value 0.005 (0.5 %) was chosen for

all fault parameters. All further calculations of the turboshaft matrix H use this value.

Figure 5 illustrates the behavior of the high pressure compressor efficiency influence coefficients of the turbofan engine. Comparing Figures 5 and 4, one can state that the influence coefficient plots of both engines are quite similar, and the variation value optimal for the turboshaft seems to be correct for the turbofan as well. The above graphical analysis of the variations was repeated for all fault parameters of both engines and the variation value 0.005 was found the best. Therefore, this value was used to determine all the matrixes H in the next subsection.

Influence of operating conditions on the matrix H

Once the optimal variation value was selected, we can compute the matrixes H of both engines. Computed at the design point, these matrices are given as an example in Table A2 of the Appendix.

To analyze the influence of the operating conditions, many operating points were determined for each engine by independently changing the relative rotation speed of HPC (power set variable) from 1 to 0.72 and the ambient temperature in a range 264 to 312 K. Figure

6 shows on a turboshaft compressor map the simulated operating points with different rotation speed values. For each value of the speed or temperature, the fault influence matrix H was computed using a fixed variation 0.005 for each of the six fault parameters. Table A3 illustrates the set of the temperature values and the re-

sulting turboshaft fault influence coefficients. Once the matrixes H were calculated under different operating conditions, we can plot the influence coefficients against each condition variable, HPC spool speed or ambient temperature, and analyze their behavior.
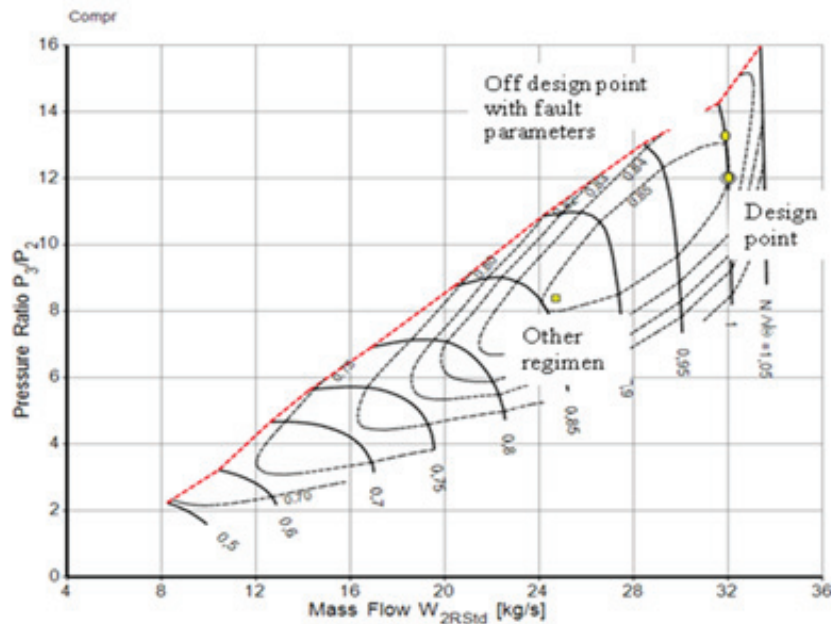

Figure 3. Design and off-design conditions during engine operation simulations by GasTurb 12 (GasTurb GmbH, 2015)
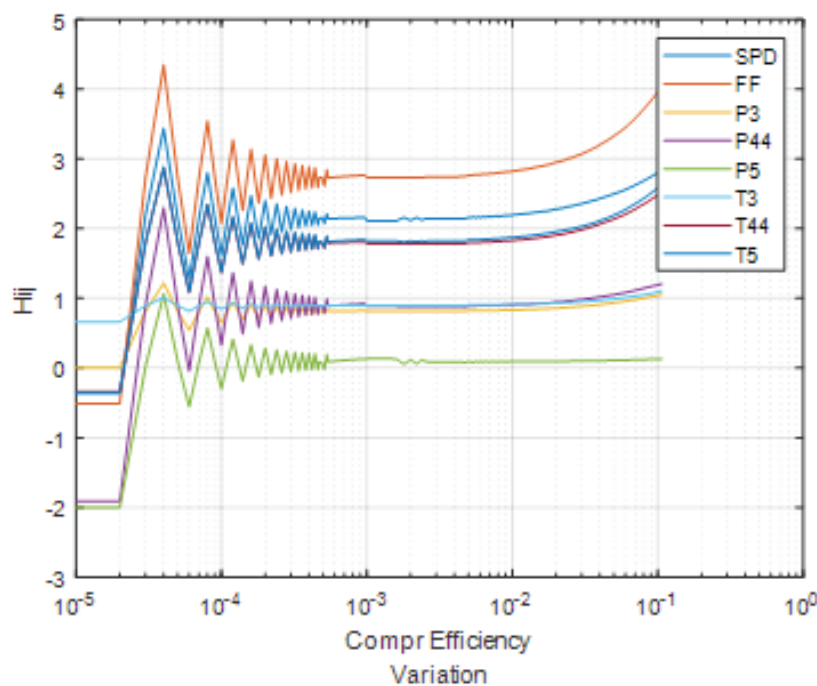

Figure 4. Selection of the optimal value of the compressor efficiency variation (turboshaft)
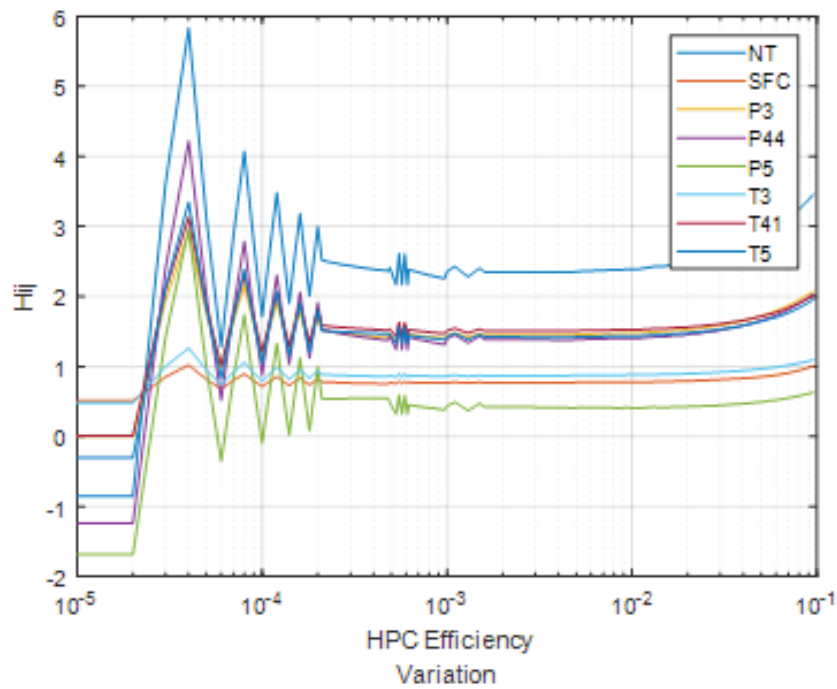
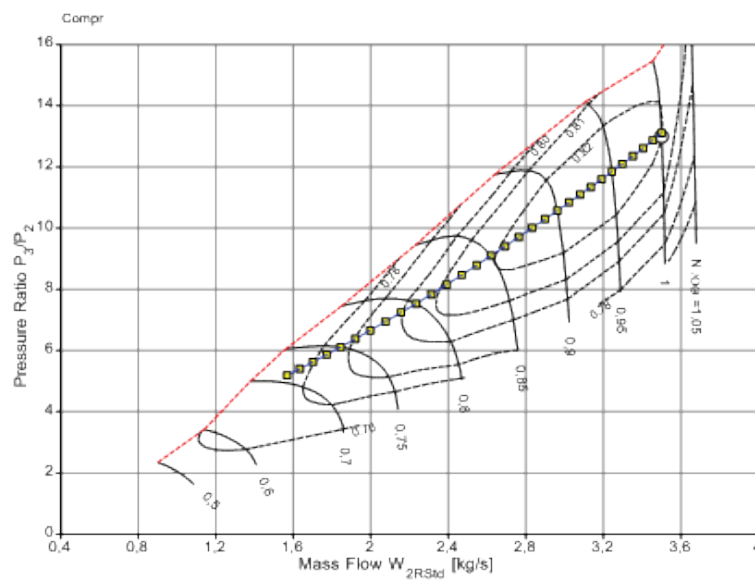Figure 5. Selection optimal value of the HPC efficiency variation (turbofan)

Figure 6. Turboshaft simulated operating points (GasTurb GmbH, 2015)

Figures 7, 8, 9 and 10 illustrate the behavior of the fault influence coefficients of both engines. As before, the influence coefficients of compressor efficiency are presented. They are plotted against each operating condition. Using the plots presented, let us firstly analyze possible random errors in the influence coefficients and then evaluate general trends in these coefficients. It can be seen in Figures 7 and 8 that the change of the HPC spool speed does not cause random point-to-point errors, and irregularities in the behavior of the influence coefficients are rare and small. As to Figures 9 and 10 where the input temperature varies, some low level random errors are observed in the right side of the figures. In general, all irregularities and errors are smaller than those in Figure 1, and the coefficients change more gradually.

General behavior of the influence coefficients depends on a particular variable of operating conditions. The rotation speed has a significant impact. As is shown in Figures 7 and 9, the influences coefficients depend significantly on the speed for both engines, and this dependence is strongly nonlinear. For the turboshaft, the dependence has different directions: the coefficients mainly grow on left side of Figure 7 and their curves descend on the right side. In contrast, the turbofan coefficients constantly grow (Figure 9). As to the input temperature, Figures 8 and 10 show that its impact is by far lower, and the coefficients change lineally and slowly or remain constant.
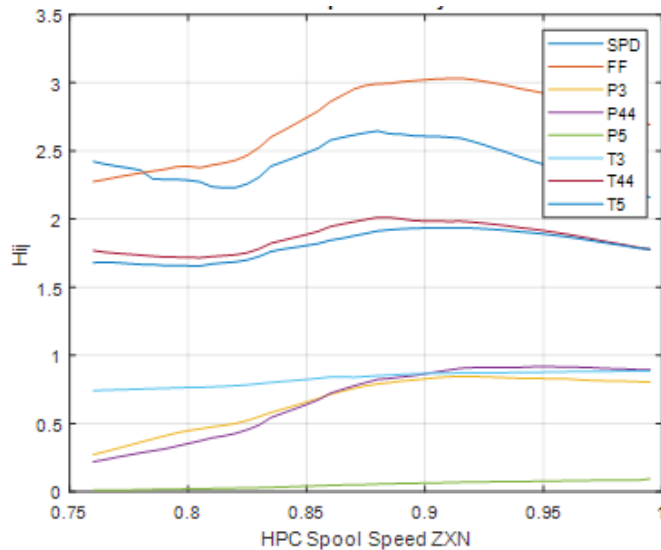

Figure 7. Compressor efficiency influence coefficients vs HPC spool speed (turboshaft)
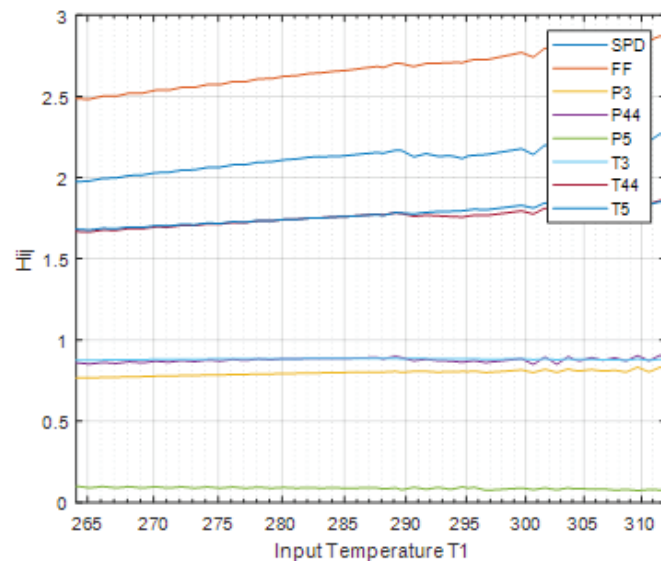

Figure 8. Compressor efficiency influence coefficients vs input temperature (turboshaft)
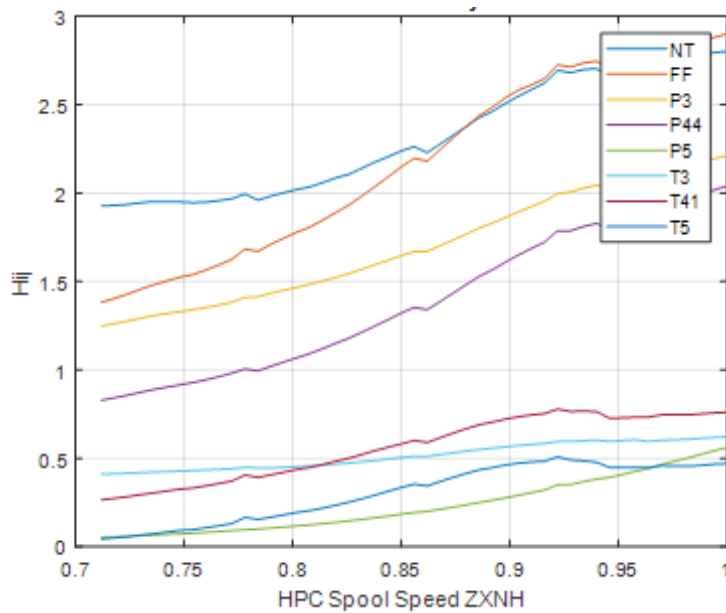
Figure 9. HPC efficiency influence coefficients vs HPC spool speed (turbofan)
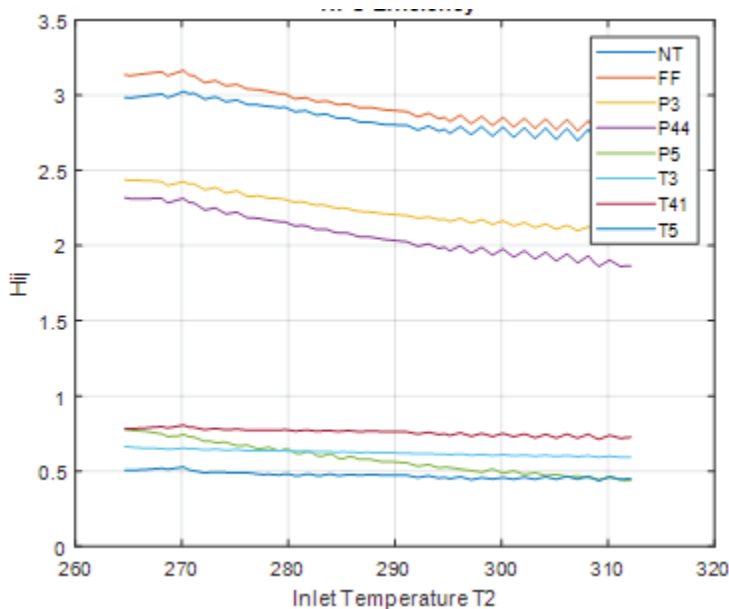

Figure 10. HPC efficiency influence coefficients vs input temperature (turbofan)

The next section deals with the operating condition influence matrix G. As with the matrix H, the optimal variation value is determined first, and then the influence of operating conditions on this matrix is analyzed.

ANALYSIS OF THE OPERATING CONDITION INFLUENCE MATRIX G

OPTIMAL VARIATION OF OPERATING CONDITIONS

The optimal value of the variation of operating conditions corresponds to the most accurate calculation of the matrix G. As with the matrix H, we compute the matrix G with different variation values and analyze the plots of the influence coefficients G_{ij} against a variation value. These plots constructed for both engines are shown in Figures 11 and 12 for the HPC spool speed (first operating condition) and in Figures 13 and 14 for the input temperature (second operating condition). As before, we look for the intervals where the coefficients are constant and choose in this intervals the optimal variation value. By doing so for all of the matrix G coefficients, we selected the optimal value 0.005 that is used
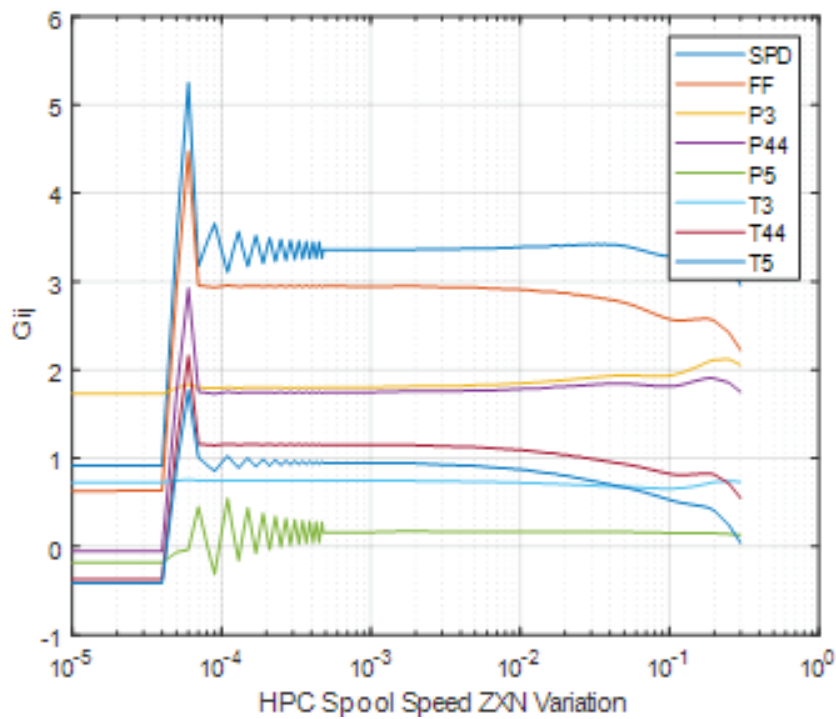
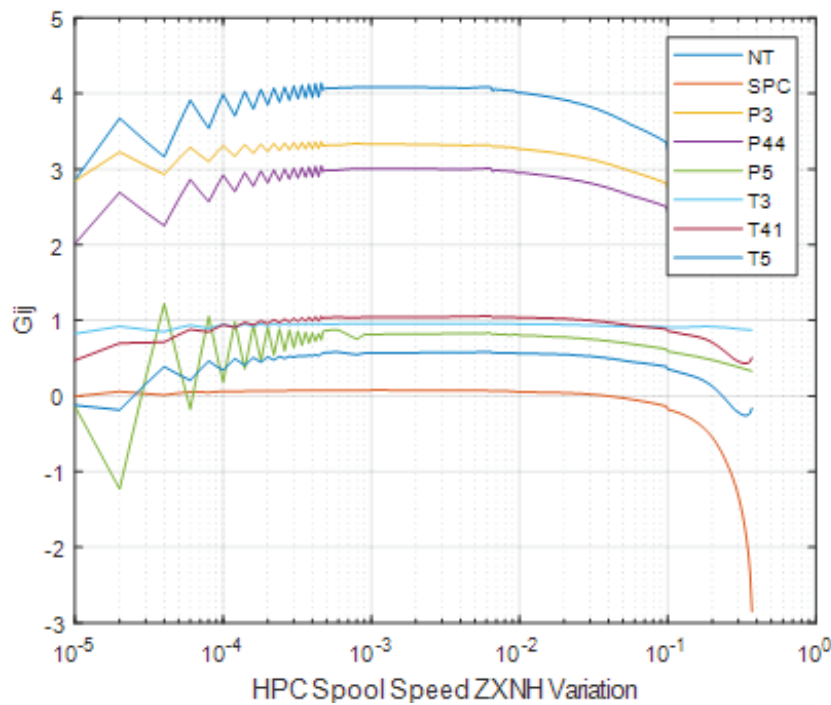Figure 11. Selection of the optimal variation value of HPC spool speed for the turboshaft

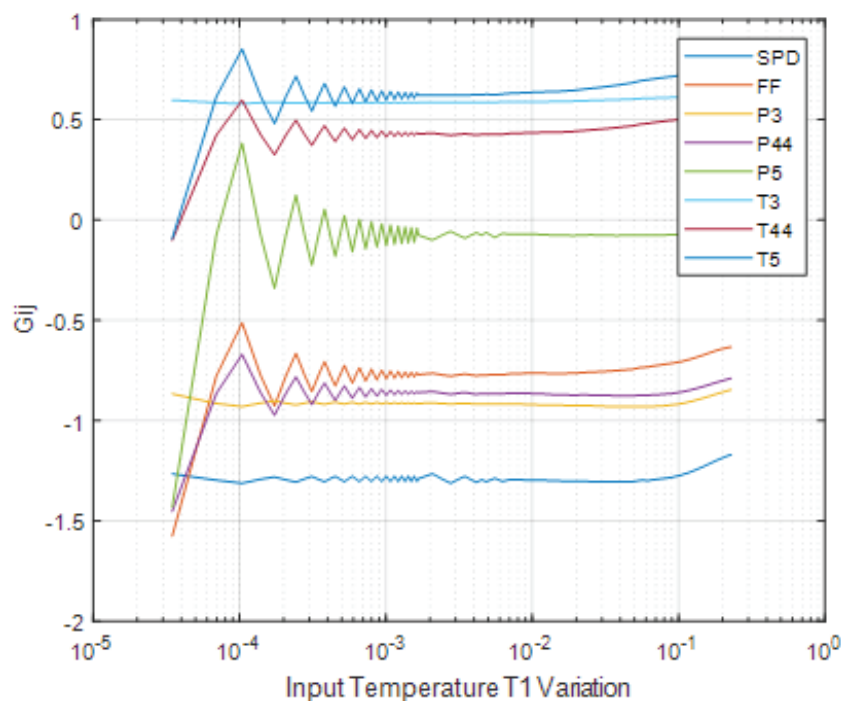Figure 12. Selection of the optimal variation value of HPC spool speed for the turbofan

Figure 13. Optimal variation of input temperature for the turboshaft
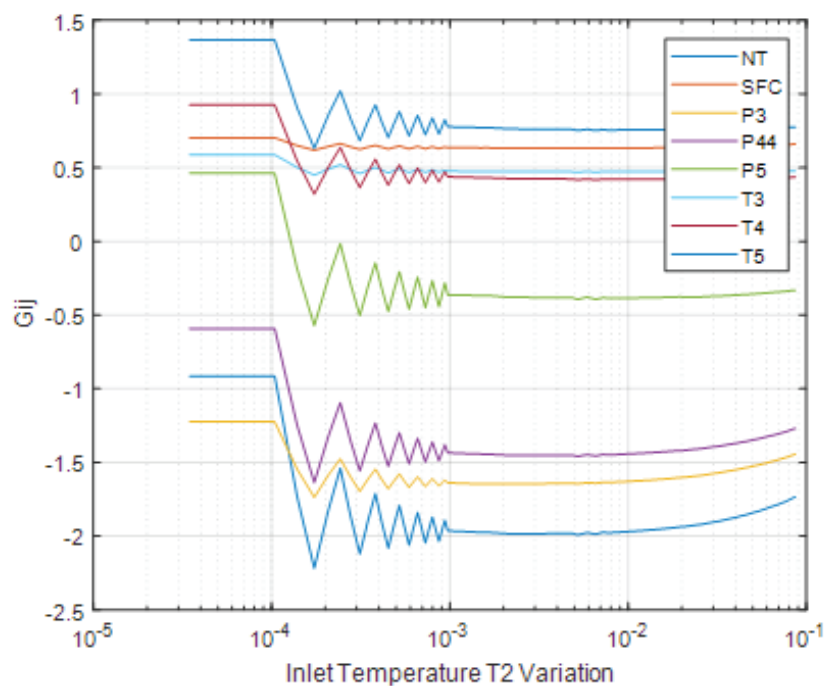

Figure 14. Optimal variation of input temperature for the turbofan

in all of the further calculations of the matrix G. Table A4 of the Appendix exemplifies the operating condition influence matrices by presenting the influence coefficients obtained at the design point.

INFLUENCE OF OPERATING CONDITIONS ON THE MATRIX G

Figures 15 and 17 for the turboshaft and Figures 16 and 18 for the turbofan illustrate the behavior of the influence coefficients of the matrix G under varying operating conditions, a HPC spool speed and an engine input temperature. We can see in these figures that the coefficients behavior is gradual and does not manifest per-

turbations and random faults. Additionally, it follows from Figures 15 and 16 that the impact of the rotation speed is now small and lineal. In contrast, the input temperature variations cause now more significant and nonlinear changes of the coefficients.

Summing up the results of sections 3 and 4, we can draw the following conclusions. First, random errors of the matrix H are rare and small, and they are practically absent in the calculation of the matrix G. Second, general changes of the matrixes H and G because of varying operating conditions can be significant. Third, when the operating conditions vary, the behavior of the coefficients of the matrixes H and G is quite different.
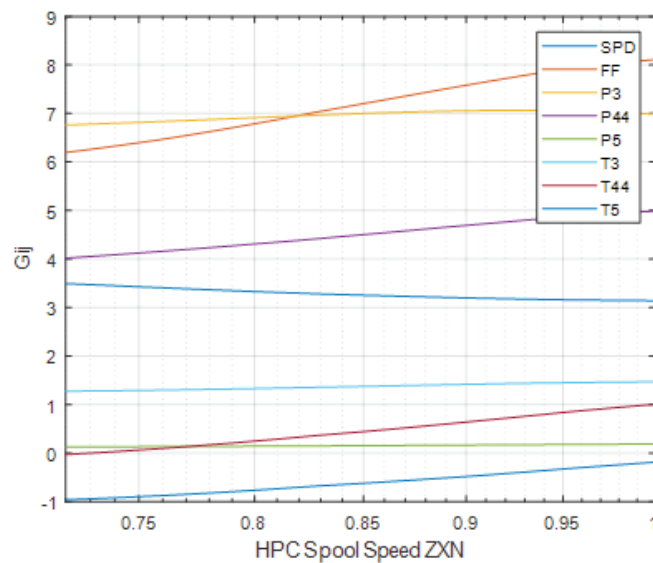

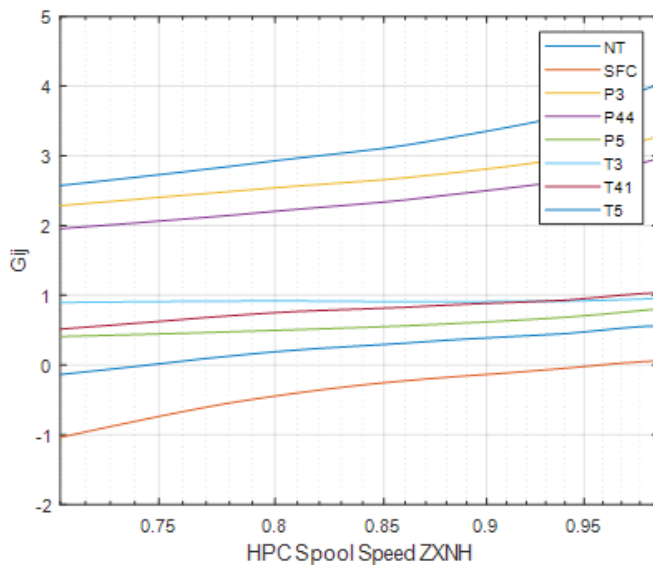Figure 15. Influence of HPC spool speed on the matrix G coefficients for the turboshaft

Figure 16. Influence of HPC spool speed on the matrix G coefficients for the turbofan
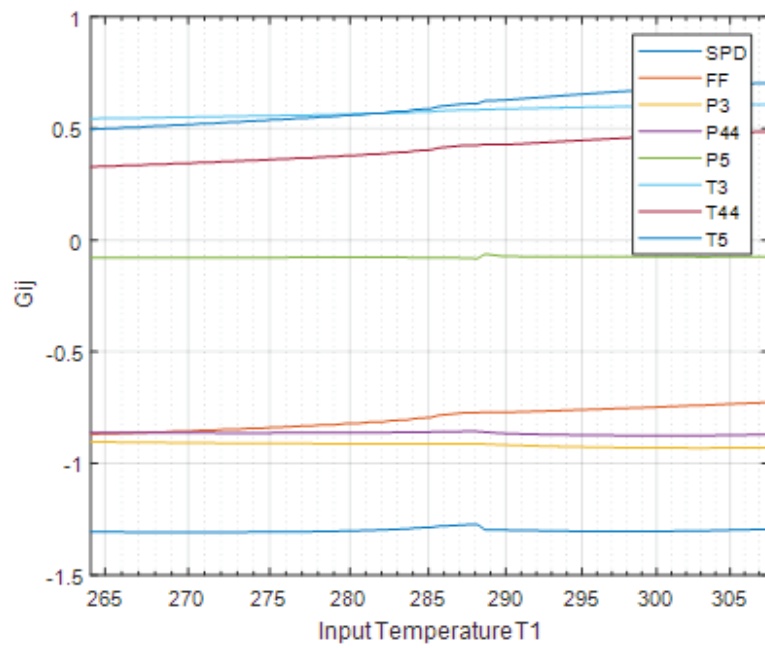
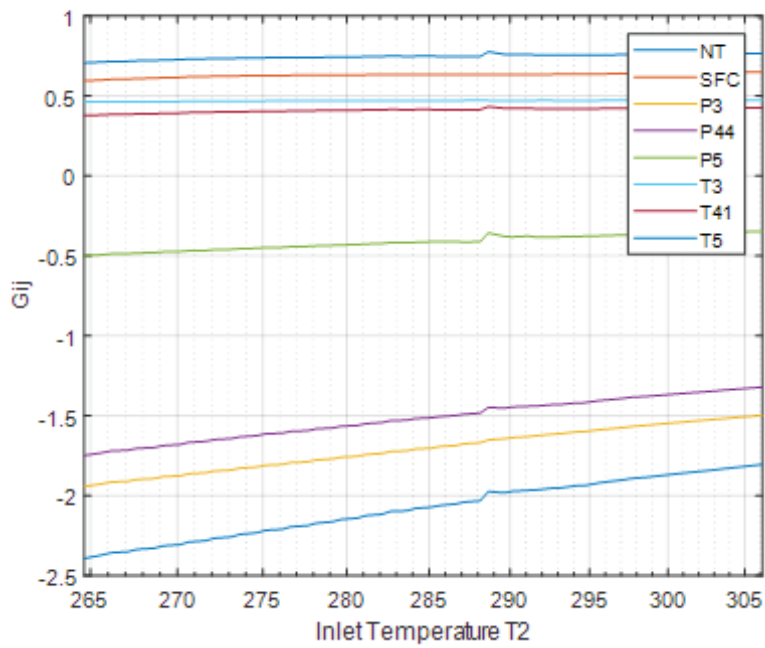Figure 17. Influence of input temperature on the matrix G coefficients for the turboshaft

Figure 18. Influence of the input temperature on the matrix G coefficients for the turbofan

Conclusions

The fault and operating condition influence matrices were computed and analyzed based on the underlying nonlinear thermodynamic models of a turboshaft and a turbofan from the GasTurb 12 software. Comparing the actual results in Figures 4 and 5 and Table A2 with the previous results of Figure 2, one can note that the intervals of fault coefficient changes do not considerably differ. These differences are well explained by different engines analyzed and different variable employed to set power during matrix computation. Comparing now the nonlinearity effects observed in Figures 4 and 5 with those presented en Figures 1 to 3 in (Kamboukos & Mathioudakis, 2005), we can conclude that the present and cited papers point out very similar effects of increasing nonlinearity when a fault parameter variation grows. Thus, the results of the present paper do not contradict to previous information.

As shown in Figures 4, 5, 11-14, the selection and use of the optimal variation value of fault parameters and operating conditions resulted in vanishing linearization and random errors in the influence coefficient calculations. Hence, any fluctuations in the behavior of these coefficients, if any, mean internal inaccuracy of the underlying models i.e. the influence coefficients become indicators of the thermodynamic model accuracy.

The analysis of influence matrixes, which were computed for a turboshaft and turbofan using GasTurb 12, has shown that these matrixes have significantly smaller fluctuations compared with the matrixes previously analyzed. In this way, GasTurb 12 can be used as an accuracy pattern to enhance thermodynamic models of another origin.

The analysis of the influence matrices also helps to draw another important conclusion that the influence coefficients can significantly change when operating conditions vary. This means that the diagnostic solutions based on a constant influence matrix will be less applicable, however a multipoint diagnostic option will be more useful as shown by Loboda *et al.* (2007).

Acknowledgments

Appendix

Table A1. Turboshaft compressor efficiency (CE) influence coefficients for different values of the variation

Variation of fault parameter CE	Monitoried variables							
	SPD	FF	P3	P44	P5	T3	T44	T5
−0.00001	−0.35507	−0.51153	0.00000	−1.91352	−2.00323	0.66328	−0.34368	−0.35806
−0.00002	−0.35508	−0.51154	0.00000	−1.91353	−2.00323	0.66329	−0.34368	−0.35806
−0.00003	2.19270	2.73087	0.81321	0.89552	0.02069	0.89360	1.80103	1.79863
...	...	...	...	...	...	...	...	...
−0.00095	2.15830	2.76594	0.82055	0.92026	0.12926	0.89718	1.80827	1.83990
−0.00096	2.15852	2.76644	0.82066	0.92065	0.12978	0.89722	1.80848	1.84028
−0.00097	2.15874	2.76693	0.82077	0.92103	0.13029	0.89726	1.80868	1.84066
−0.0010	2.11383	2.73066	0.81281	0.88913	0.13129	0.89503	1.78471	1.82102
−0.0011	2.11313	2.73064	0.81280	0.88848	0.13154	0.89515	1.78361	1.82108
−0.0012	2.11253	2.73069	0.81279	0.88783	0.13163	0.89526	1.78269	1.82114
...	...	...	...	...	...	...	...	...
−0.0096	2.18657	2.81836	0.83089	0.90533	0.09970	0.91017	1.82653	1.87178
−0.0097	2.19326	2.82031	0.83132	0.90657	0.09286	0.91041	1.82772	1.87159
−0.0098	2.19422	2.82164	0.83160	0.90701	0.09295	0.91061	1.82852	1.87242
−0.010	2.19540	2.82392	0.83209	0.90759	0.09356	0.91098	1.82985	1.87396
−0.011	2.20542	2.83733	0.83495	0.91218	0.09391	0.91299	1.83785	1.88228
−0.012	2.21348	2.84854	0.83733	0.91491	0.09298	0.91486	1.84444	1.88921
...	...	...	...	...	...	...	...	...
−0.105	2.81673	4.01729	1.05119	1.20271	0.12974	1.10233	2.51070	2.61991
−0.106	2.82126	4.02964	1.05302	1.20503	0.13021	1.10450	2.51711	2.62709
−0.107	2.82580	4.04179	1.05481	1.20733	0.13077	1.10667	2.52361	2.63433

Table A2. Fault influence matrices H computed at the design point (relative rotation speed 1.0 and ambient temperature 285.0 K)

Turboshaft

Monitored variables	Fault parameters					
	CC	CE	HPTC	HPTE	PTC	PTE
SPD	−2.5505	2.1552	−0.5535	2.7178	1.9263	−1.1328
FF	−2.1444	2.7657	−0.6570	3.4662	1.5816	0.0007
P3	−1.3559	0.8197	0.8182	0.8560	0.3914	0.0002
P44	−1.3541	0.8916	−0.2365	1.1234	1.4366	0.0006
P5	−0.1261	0.0955	−0.0221	0.1131	0.0437	0.0149
T3	−0.4052	0.9016	0.2325	0.2432	0.1111	−0.0000
T41	−0.7585	1.7961	−0.4190	2.2559	1.0315	0.0004
T5	−0.5861	1.8372	−0.4121	2.3030	0.8634	0.3120

Turbofan

Monitored variables	Fault parameters					
	LPCC	HPCC	HPCE	HPTC	HPTE	-
NT	−2.8029	−1.1072	2.3548	2.9986	2.5321	-
SFC	−0.0996	−0.3076	0.7709	0.9493	0.1100	-
P3	−2.2120	0.3294	1.4545	1.7211	1.3104	-
P44	−2.0400	−0.6733	1.3840	1.7641	2.1504	-
P5	−0.5608	−0.1899	0.4088	0.5175	0.3571	-
T3	−0.6217	0.0941	0.8708	0.4607	0.3498	-
T41	−0.7608	−0.4683	1.5099	1.6585	1.0275	-
T5	−0.4703	−0.6020	1.4220	1.7919	0.8698	-

Table A3. Turboshaft compressor efficiency (CE) influence coefficients for different values of the input temperature

Input temperature T1 (°C)	Monitoried variables							
	SPD	FF	P3	P44	P5	T3	T44	T5
264.15	1.97380	2.48516	0.76621	0.86067	0.09992	0.87453	1.66856	1.68270
264.65	1.97671	2.48398	0.76643	0.85621	0.09473	0.87486	1.66709	1.67985
265.15	1.97929	2.48278	0.76664	0.85180	0.08958	0.87519	1.66562	1.67712
...	...	...	...	...	...	...	...	...
311.15	2.24617	2.85766	0.81807	0.88960	0.07780	0.87803	1.84827	1.84311
311.65	2.27094	2.87244	0.83289	0.90714	0.07674	0.88203	1.85993	1.85190
312.15	2.25138	2.85958	0.81735	0.89039	0.07833	0.87726	1.85277	1.84762

Table A4. Operating condition influence matrices G computed at the design point (relative rotation speed 1.0 and ambient temperature 285.0 K)

	Turboshaft			Turbofan		
Monitored variables	Operating conditions		Monitored variables	Operating conditions	
	T1	ZXN		T2	ZXNH
SPD	−1.2964	3.3580	NT	−1.9808	4.0853
FF	−0.7779	2.9433	SFC	0.6314	0.0691
P3	−0.9142	1.8031	P3	−1.6408	3.3153
P44	−0.8650	1.7476	P44	−1.4505	3.0095
P5	−0.0751	0.1616	P5	−0.3817	0.8303
T3	0.5840	0.7447	T3	0.4716	0.9581
T41	0.4227	1.1492	T41	0.4224	1.0576
T5	0.6147	0.9662	T5	0.7587	0.5846

References

Fentaye, A. D., Baheta, A. T., Gilani, S. I. & Kyprianidis, K. G. (2019). A review on gas turbine Gas-Path diagnostics: State of the art methods, challenges and opportunities. *Aerospace.* https://doi.org/10.3390/aerospace6070083

GasTurb GmbH. (2015). Design and Off-Design performance of gas turbines. GasTurb 12, 294p.

Jardine, A. K., Banjevic, D. & Daming, L. (2006). A review on machinery diagnostics prognostics implementing condition based maintenance. *Mechanical Systems and Signal Processing*, 1483-1510. https://www.researchgate.net/deref/http%3A%2F%2Fdx.doi.org%2F10.1016%2Fj.ymssp.2005.09.012

Kamboukos, P. & Mathioudakis, K. (2005). Comparison of linear and non linear gas turbine performance diagnostics. *Journal of Engineering for Gas Turbines and Power*, 49-56. https://doi.org/10.1115/1.1788688

Li, Y. G. (2002). Performance-analysis-based gas turbine diagnostics. *IMechE*, 366 - 376. http://dx.doi.org/10.1243/095765002320877856

Loboda, I., Feldshteyn, Y. & Yepifanov, S. (2007). Gas turbine diagnostics under variable operating conditions. International Technical Congress Power for Land Sea & Air (p. 6P). Montreal, Canada: ASME.

North Atlantic Treaty Organisation. (2002). Performance prediction and simulation of gas turbine engine operation. RTO Technical Report 44, 1, 3-39, 40, 47.

Pinelli, M. & Spina, P. R. (2002). Gas Turbine field performance determination: Sources of uncertainties. *Journal of Engineering for Gas Turbines and Power*, 155-160. https://doi.org/10.1155/2012/142173

Sampath, S. & Singh, R. (2005). An integrated fault diagnostics model using genetic algorithm and neural networks. *Journal of Engineering for Gas Turbines and Power*, 49-56. https://doi.org/10.1115/1.1995771

Tahan, M., Tsoutsanis, E., Muhammad, M. & Adbul Karim, Z. (2017). Performance based health monitoring, diagnostics and prognostics for condition based maintenance of gas turbines: A review. *Applied Energy*, 198, 122 -144.

Urban, L. (1973). Gas path analysis applied to turbine engine condition monitoring. *J. Airc.*, 10, 400-406. https://doi.org/10.2514/3.60240

Vanini, Z., Khorasani, K. & Meskin, N. (2014). Fault detection and insolation of a dual spool gas turbine engine using dynamic neural networks and mutiple model approach. *Information Sciences*, 234-251. https://doi.org/10.1016/j.ins.2013.05.032